Structure and Conformational Stability of a Tetrameric Thermostable *N*-Succinylamino Acid Racemase

Joaquín Pozo-Dengra,[1] Sergio Martínez-Rodríguez,[1] Lellys M. Contreras,[2] Jesús Prieto,[3] Montserrat Andújar-Sánchez,[1] Josefa M. Clemente-Jiménez,[1] Francisco J. Las Heras-Vázquez,[1] Felipe Rodríguez-Vico,[1] José L. Neira[4,5]

[1] *Departamento de Química Física, Bioquímica y Química Inorgánica, Universidad de Almería, 04120 Almería, Spain*

[2] *Departamento de Biología, Facultad Experimental de Ciencias y Tecnología, Universidad de Carabobo, 2001 Valencia, Venezuela*

[3] *Structural Biology and Biocomputing Programme, Centro Nacional de Investigaciones Oncológicas (CNIO), 28007 Madrid, Spain*

[4] *Instituto de Biología Molecular y Celular, Universidad Miguel Hernández, 03202 Elche (Alicante), Spain*

[5] *Biocomputation and Complex Systems Physics Institute, 50009 Zaragoza, Spain*

Received 29 December 2008; revised 8 April 2009; accepted 9 April 2009
Published online in Wiley InterScience (www.interscience.wiley.com). DOI 10.1002/bip.21226

ABSTRACT:

The N-succinylamino acid racemases (NSAAR) belong to the enolase superfamily and they are large homooctameric/hexameric species that require a divalent metal ion for activity. We describe the structure and stability of NSAAR from Geobacillus kaustophilus (GkNSAAR) in the absence and in the presence of Co^{2+} by using hydrodynamic and spectroscopic techniques. The Co^{2+}, among other assayed divalent ions, provides the maximal enzymatic activity at physiological pH. The protein seems to be a tetramer with a rather elongated shape, as shown by AU experiments; this is further supported by the modeled structure, which keeps intact the largest tetrameric oligomerization interfaces observed in other homooctameric members of the family, but it does not maintain the octameric oligomerization interfaces. The native functional structure is mainly formed by α-helix, as suggested by FTIR and CD deconvoluted spectra, with similar percentages of structure to those observed in other protomers of the enolase superfamily. At low pH, the protein populates a molten-globule-like conformation. The GdmCl denaturation occurs through a monomeric intermediate, and thermal denaturation experiments indicate a high thermostability. The presence of the cofactor Co^{2+} did alter slightly the secondary structure, but it did not modify substantially the stability of the protein. Thus, GkNSAAR is one of the few members of the enolase family whose conformational propensities and stability have been extensively characterized. *Biopolymers 91: 757–772, 2009.*
Keywords: N-succinylamino acid racemase; protein stability; protein structure; tetramer; fluorescence; enolase superfamily

Additional Supporting Information may be found in the online version of this article.
Correspondence to: José L. Neira; e-mail: jlneira@umh.es
Contract grant sponsor: Spanish Ministerio de Educación y Ciencia
Contract grant numbers: SAF2008-05742-C02-01, CSD2008-00005
Contract grant sponsor: Spanish Ministerio de Educación y Ciencia
Contract grant number: BIO2007-67009
Contract grant sponsor: Andalusian Consejería de Innovación, Ciencia y Tecnología
Contract grant number: P07-CVI-2651
Contract grant sponsor: FIPSE association
Contract grant number: Exp 36557/06
Contract grant sponsor: Fondo Nacional para la Ciencia y Tecnología de Venezuela
Contract grant number: Pem 2001002268
Contract grant sponsor: Consejo de Desarrollo Científico y Humanístico, Universidad de Carabobo
Contract grant number: 058-06
Contract grant sponsor: Generalitat Valenciana (Ayudas a investigadora invitada)
Contract grant number: AINV06/102
Contract grant sponsor: Ministerio de Educación y Ciencia (Estancia de jóvenes doctores extranjeros en España
Contract grant number: SB2005-0011

This article was originally published online as an accepted preprint. The "Published Online" date corresponds to the preprint version. You can request a copy of the preprint by emailing the Biopolymers editorial office at biopolymers@wiley.com

INTRODUCTION

Enantiomerically pure α-amino acids are important products with applications in the pharmaceutical, food, feed, and agrochemical industries[1]; further, non-natural amino acids are intermediate reagents during the synthesis of antibiotics and pesticides.[2] Some L-amino acids can be obtained on a large scale by using microbial biosynthesis, but other D-enantiomeric compounds are obtained by enzymatic synthesis from available precursors. There are several enzymatic processes for production of amino acids, such as the hydantoinase[3] or the amidase methods.[4,5] An alternative approach uses L-acylases, which catalyze the transformation of a mixture of *N*-acetyl-D,L-amino acids into L-amino, and *N*-acetyl-D-amino acids. The isolated *N*-acetyl-D-amino acids are racemized under drastic conditions (high pH and temperature) and, then, returned to the initial reaction.[6] It is clear, then, that the use of an enzymatic racemization of the nonhydrolysed D,L-acetylamino acids could make cheaper the whole industrial process, since the racemization and separation steps would not be longer required.

N-acylamino acid racemase, or *N*-succinylamino acid racemase as it has also recently described[7] (NSAAR), allows the racemization of *N*-acetylamino acids under physiological conditions. NSAARs belong to the enolase superfamily; they have been isolated from several organisms,[8–13] and the three-dimensional structure of the NSAAR from *Deinococcus radiodurans* (DrNSAAR) has been solved.[14] The biochemical characterization of other members of the family indicates that: (i) NSAARs act on a broad range of *N*-acetylamino acids; (ii) they need a divalent metal ion for its function (to polarize a C-H bond adjacent to a carboxylate group for abstraction of the hydrogen by a basic residue of the enzyme); and (iii) they are homooctameric or homohexameric species.[8,10,12–14] Enzymes from thermostable microorganisms have attracted much attention because of their intrinsic high thermal stability and large reaction rates[15]; besides, the use of high temperatures during the industrial enzymatic reactions increases the mass transfer effects, improves the solubility of substrates in water and reduces the possibility of cross-contaminations.[16] Within this framework, we are trying to isolate a new NSAAR with a wide potential use in industrial processes. The complete genomes of twenty thermophilic or hyperthermophile prokaryotic species have been described.[17] *Geobacillus kaustophilus*, a thermophilic *Bacillus*-related species, is among those genome-sequenced organisms. Its genome is composed of a 3.54 Mb single circular chromosome and a 47.9 kb plasmid. Uchiyama and coworkers[17] have assigned a biological role to 1914 of the 3498 predicted protein-coding genes, and one of them corresponds to a putative NSAAR. We have cloned the gene encoding for this protein, GkNSAAR, and we have described its biochemical properties, showing that its *N*-acylamino acid racemase activity is enhanced by cobalt-ions.[18]

In this work, we report the structure, stability, and oligomerization state of GkNSAAR at different pH and temperatures, in the absence and in the presence of Co^{2+}, by using spectroscopic (namely, fluorescence, CD, and FTIR), and hydrodynamic (AU) techniques. The results indicate that GkNSAAR is a tetramer at pH 8.0, as shown by AU, within a wide pH range (from pH 5.3 to 9.0), but the functional tertiary and secondary structures are only present within a very narrow pH range (from pH 7.0 to 9.0). In GdmCl denaturation experiments, the folding reaction proceeds *via* a monomeric intermediate with non-native structure. Upon addition of Co^{2+}, small changes were observed in the amount of secondary structure, but the tertiary and quaternary ones were not altered; further, the stability of the protein was not modified by the presence of the metal. Thus, although enzyme activity is linked to the presence of the Co^{2+}, the ion only seems to alter slightly the amount of secondary structure.

RESULTS

GkNSAAR is a Tetrameric Species Either in the Presence or in the Absence of Co^{2+}

We used gel filtration and AU techniques to elucidate the quaternary structure of GkNSAAR.

Gel Filtration Measurements. GkNSAAR, whether or not the ion was present, eluted at 19.64 ml in a Superdex 200 HR 16/60 column (close to the bed volume of the column) at pH < 7.5 and pH > 10 (data not shown). These results, with those from AU (see latter), suggest that the protein probably interacted with the column at those pH (see also Discussion section). The protein eluted at 10.94 ml (with a $\sigma = 0.21$) in the pH range 7.5–9.0, which yields a R_s of 46.7 Å (Figure 1A). This elution volume is close to the peak of aldolase (R_s 48.1 Å), which is a tetramer composed of subunits of ~360 amino acids (the GkNSAAR monomer is formed by 379 amino acids, with a molecular weight of 42.3 kDa). Since

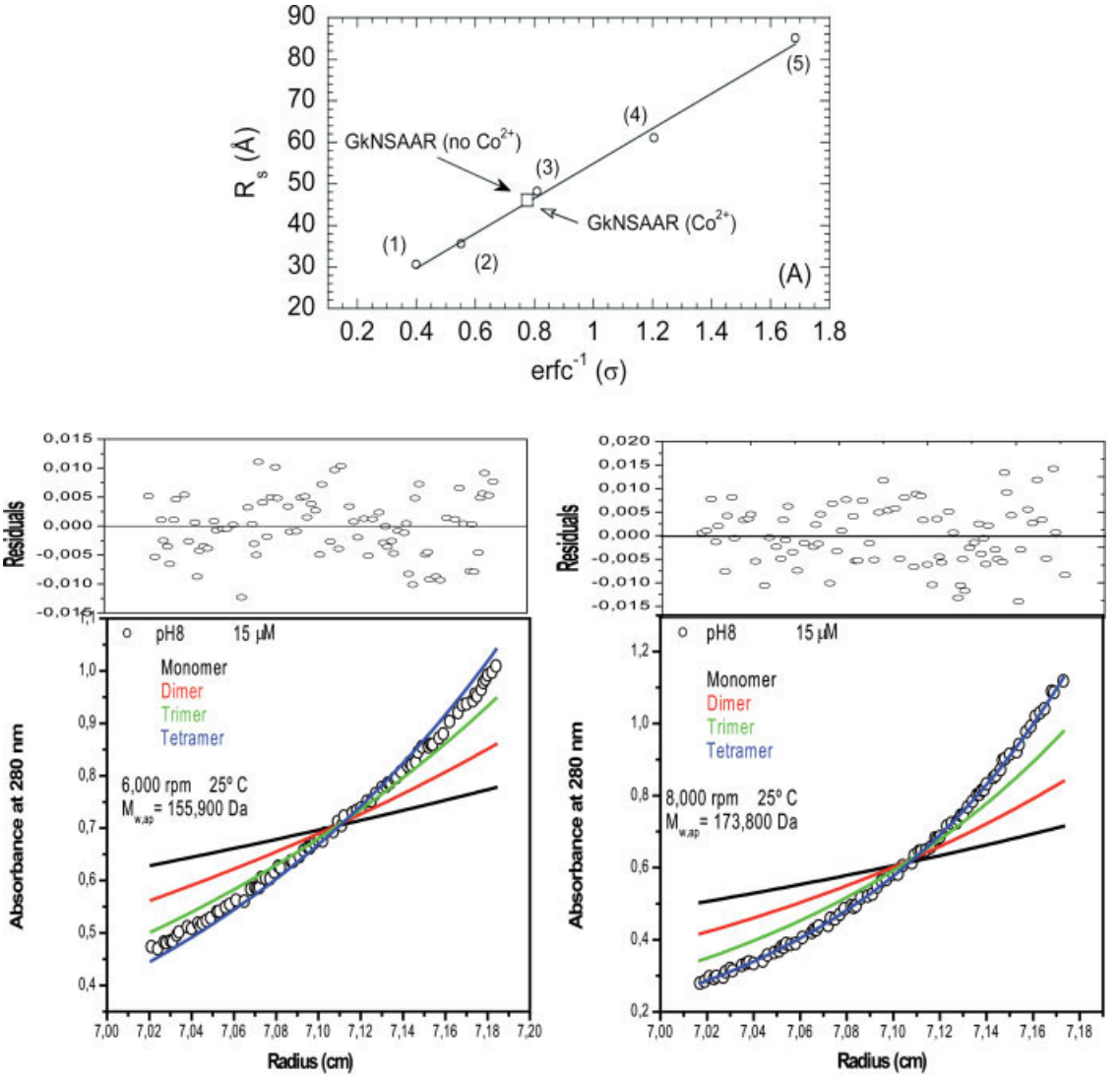

FIGURE 1 Hydrodynamic properties of GkNSAAR. A: Determination of the Stokes radius of GkNSAAR at pH 8.0. The elution volume of the protein in the absence of Co^{2+} is indicated by a filled arrow, and that in the presence of 0.5 m*M* Co^{2+} by a blank arrow (both proteins eluted at the same volume, and then the two rectangles are superimposed). The numbering corresponds to the elution volumes of ovalbumin (1), albumin (2), aldolase (3), ferritin (4), and thyroglobulin (5). The equation was: $R_s = 41.6 \times \text{erfc}^{-1}(\sigma) + 7.39$ (with a regression coefficient of 0.99). B: Sedimentation equilibrium data at pH 8.0. The upper graphs are the distribution of residuals calculated by subtracting the fitted values from observed data for the tetramer molecular mass provided by the program EQASSOC,[19] that is, the residuals correspond to deviation of the experimental data from the theoretically calculated tetrameric mass. Absorbance data taken at 15 μM of GkNSAAR loading concentration are shown in the lower graph versus cell radius at 6000 (left) and 8000 (right) rpm, 298 K. Open white rings show the experimental data, and color solid lines are the fitting to four equilibria involving different final oligomeric states of GkNSAAR.

for spherical proteins $\log(R_s) = -0.204 + 0.357 \log(M_w)$,[20] this yields a $M_w = 177.3$ kDa, slightly higher than that of a tetrameric species (169.2 kDa). The elution volume did not change in 1–76.45 μM GkNSAAR concentration range explored (data not shown).

Analytical Ultracentrifugation. The results from gel filtration suggest the presence of an elongated tetrameric species in solution. Gel filtration cannot distinguish contributions of mass and shape to molecular diffusion. Conversely, AU can be used to determine directly the molar mass of the associa-

tion state of macromolecules.[21] Then, the oligomeric state of GkNSAAR, whether or not the ion was present, was also investigated by sedimentation equilibrium at three different pH.

We carried out AU experiments at equilibrium[21,22] to provide a good estimate of the oligomerization state of GkNSAAR. The sedimentation equilibrium experiments with GkNSAAR suggest the presence of a tetramer at the three pH explored (with apparent molecular weights of 156 kDa at 6000 rpm) (Figure 1B, left-hand side). At higher velocities (8000 and 10,000 rpm), fitting of the data yields a molecular mass of 170 kDa, which is similar to the expected tetrameric molecular weight (169.2 kDa) (Figure 1B, right-hand side).

We also carried out ITC measurements to determine the affinity of metals by the protein (Supporting Information Figure 1). If we assume that all the binding sites in each monomer are identical, the number of binding sites will provide us with an estimation of the stoichiometry of the complex, and then, with its geometry. The results indicate that the affinity is very large, and then, there is no baseline in the lower part of the sigmoidal curve (Supporting Information Figure 1). Thus, the affinity constant is very well determined, but not the number of binding sites, that is, the inflexion point of the curve. The fitting to four metal ions was better (smaller residuals) than that to two (data not shown) or three binding sites (Supporting Information Figure 1), but even so, the error in the calculation was large. Keeping in mind this caveat, we can consider that the ITC results, when taken together with the rest of the techniques, support unambiguously the presence of a tetrameric species for GkNSAAR.

To sum up, the results from gel filtration and AU indicate that GkNSAAR is a tetramer under equilibrium conditions, with a rather elongated shape.

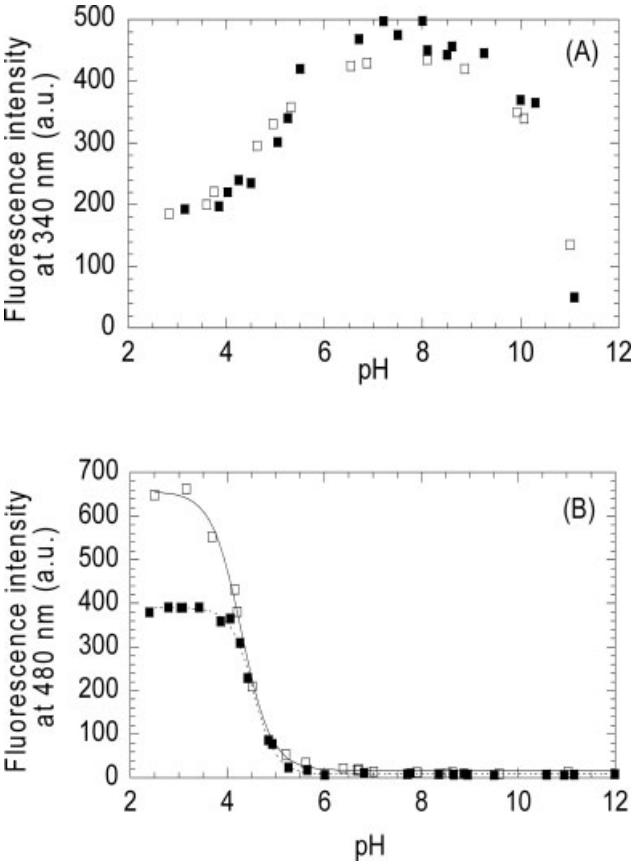

FIGURE 2 pH-Induced structural changes of GkNSAAR followed by fluorescence. A: The intensity at 340 nm in the absence (blank squares) and in the presence (filled squares) of Co^{2+}. Excitation wavelength was 280 nm (similar results were obtained by excitation at 295 nm). B: The intensity at 480 nm in ANS-fluorescence experiments in the absence of Co^{2+} (blank squares) and in the presence of 0.5 m*M* Co^{2+} (filled squares). The lines are the fitting of data to the acid-base equilibrium equation. The temperature was 298 K, and protein concentration was 1 μM.

Structure of GkNSAAR Either in the Absence or in the Presence of Co^{2+}

We used several spectroscopic probes to monitor the conformational changes in GkNSAAR, whether or not the ion was present, as the pH was modified.

Intrinsic Fluorescence. Fluorescence reports on the changes in the tertiary structure of the protein around its eight tryptophans and 10 tyrosines. The emission fluorescence spectrum of GkNSAAR, whether or not the ion was present, had a maximum at 340 nm at neutral pH, and then, it was dominated by the emission of tryptophan residues. It has been suggested that tryptophan residues that emit at 340 nm are fully exposed to external quenchers, but have restricted mobility.[23] As the pH varied, the maxima wavelengths of the spectra were red-shifted toward 350 nm, suggesting that the environment of some residues could be affected by: (i) the titration of close charged groups; (ii) conformational changes in the proteins; or (iii) both phenomena.

The intensity at 340 nm (either by excitation at 280 or 295 nm) showed, whether or not the ion was present, a bell-shaped behavior with two titrations at the two extremes of pH (Figure 2A). The pK_a of the acidic titrations were 4.72 $\pm$ 0.06 (no Co^{2+}, blank squares) and 4.83 $\pm$ 0.07 (when the ion was present, filled squares); however, the titration at basic pH could not be reliably determined because of the absence of baseline. Those pK_a values suggest the presence of two titrations occurring at low pH, probably related to Asp and/or Glu residues.[24]

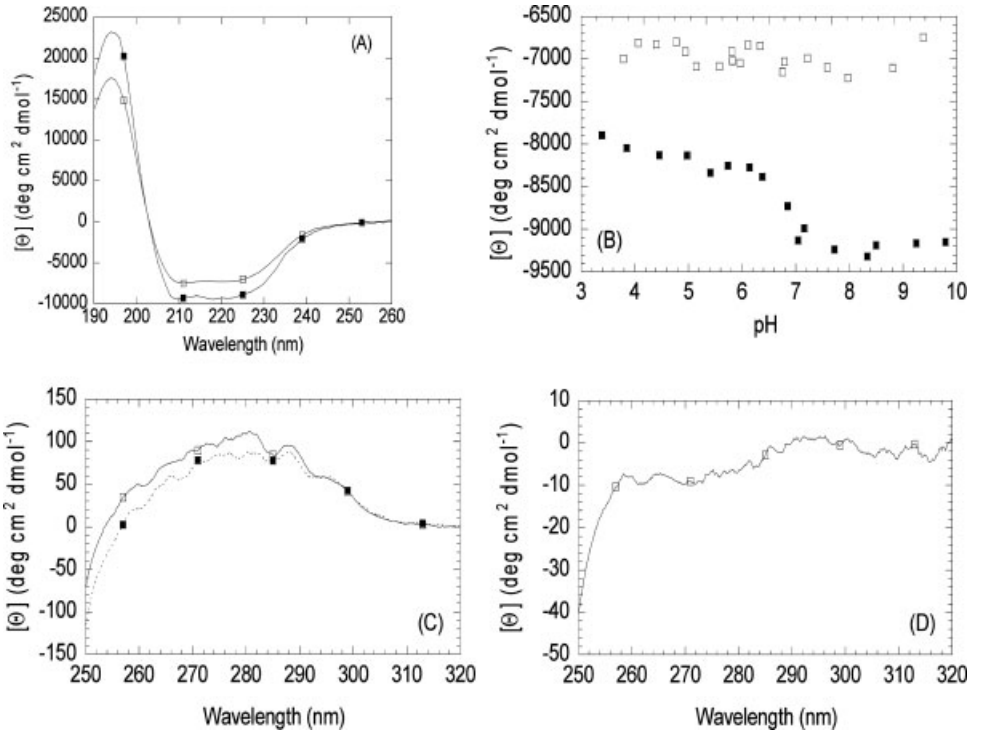

FIGURE 3 pH-Induced structural changes of GkNSAAR followed by CD. A: Far-UV steady-state spectra in the absence (filled squares) and in the presence of 0.5 m*M* Co^{2+} (blank squares) at pH 8.0. B: Changes in the molar ellipticity at 222 nm as the pH was varied in the presence (blank squares) and in the absence (filled squares) of 0.5 m*M* Co^{2+}. C: Near-UV steady-state spectra in the absence (filled squares, continuous line) and in the presence of 0.5 m*M* Co^{2+} (blank squares, dotted line) at pH 8.0. D: Near-UV CD steady-state spectrum in the absence of Co^{2+} at pH 3.7. The temperature was 298 K, and protein concentration was 1 μM for the far-UV and 15 μM for the near-UV CD.

ANS-Binding. ANS-binding was used to monitor the solvent-exposed hydrophobic regions.[25] At low pH whether or not the ion was present, the fluorescence intensity at 480 nm was large and decreased as the pH was raised (Figure 2B). This intensity showed a sigmoidal behavior with a pK_a of 4.43 $\pm$ 0.08 (no Co^{2+}, blank squares) and 4.52 $\pm$ 0.02 (when the ion was present, filled squares), which are similar to those observed by the intrinsic fluorescence.

Far- and Near-UV CD. The far-UV spectra at pH 8.0, whether or not the ion was present, were characterized by the presence of a broad minimum between 208 and 222 nm (Figure 3A) and a maximum at 194 nm. However, in the presence of the ion (blank squares), the ellipticities were smaller than those measured in the absence of Co^{2+} (filled squares): at 222 nm and pH 8.0, the intensity was 1.25-times smaller. These data suggest that the predominant secondary structure in GkNSAAR was helical, but, it is important to keep in mind that at 222 nm, the aromatic residues also contribute to the CD spectrum.[26–29] Thus, the changes in the spectra could be due to a pair of tryptophan side chains, which can give rise to CD bands of this magnitude, but only through an exciton mechanism that yields a positive and a negative band close to 225 nm.[27,29] There is no evidence for such an exciton couplet in the far UV-CD (Figure 3A) which would originate an indentation in the spectra. Furthermore, if the Trp side chains made such large contributions in the far UV, one would also expect large near-UV changes, which are not observed (see latter). In addition to changes in secondary structure and aromatic side chains, far-UV CD is also sensitive to distortions of helices such as bends or tilting of the amide planes relative to the helix axis.[26,27] Modern methods of CD analysis, such as CDNN, can take these factors into account and give reliable secondary structure contents. Deconvolution of the spectra by CDNN[30] suggests that: (i) the protein, whether or not the ion was present, was mainly formed by α-helix; and (ii) the populations of α-helical secondary structure were altered from 35 to 30% by the presence of Co^{2+} (Table I). This predicted change in the secondary structure is small, and below the error limits of the method, but it could account, at least in part, for the decrease in the ellipticity observed experimentally upon addition of the ion Co^{2+} (Figure 3A).

Table I Secondary Structural Analysis of GkNSAAR at pH 8.0 and 298 K as Determined by FTIR and CD (in Percentage)[a]

	FTIR	CD	
Structural Assignment	No Co^{2+}	No Co^{2+}	Co^{2+}
β-Turns	3	16	17
β-Turns/loops	8		
Random coil	34	35	38
α-Helix	42	35	30
Antiparallel β-sheet		5	5
Parallel β-sheet	8	9	10

[a] There is another band at 1609 cm^{-1}, assigned to side chains; it accounts for nearly 5% of the whole area of the Amide I′ band. The percentages of secondary structure on the first column of the table do not take into account this band (see text for details).

The ellipticity at 222 nm, in the absence of the ion, showed a pH-dependent sigmoidal behavior (Figure 3B, filled squares), with a $pK_a = 6.7 \pm 0.1$, and $n = 0.7 \pm 0.2$. Conversely, in the presence of the ion, the [Θ] at 222 nm did not show a sigmoidal behavior (Figure 3B, blank squares).

Near-UV spectra give information on the asymmetric and rigid environment of the aromatic residues.[26–29] The near-UV spectra of GkNSAAR at pH 8.0, whether or not the ion was present, were very intense: they had a maximum at 280 nm, and other at 288 nm (Figure 3C), suggesting strong L_b tryptophan transitions.[29,31] However, in the presence of the ion, the spectrum was more intense (Figure 3C, blank squares), in contrast to what was observed by far-UV CD (see earlier). If we assume that the changes observed in the far-UV upon addition of the ion are due to changes in the secondary structure, then the changes in the near-UV must be due to variations in the asymmetric environment(s) of some aromatic residue(s). All these features disappeared at pH 3.7 (Figure 3D), whether or not the ion was present, indicating that at low pH, the environment of aromatic residues is not longer asymmetric.

FTIR Measurements. Deconvolution of the FTIR spectra in the absence of the ion (Table I) indicates that the protein at pH 8.0 was mainly formed by helical structure, in agreement with the CD data. It is important to note here that the band at 1609 cm^{-1}, which we considered as due to the presence of side chains, could be also assigned to β-sheet, as described by Gerwert and coworkers[32]; under this assumption, the percentages of structure in Table I would be slightly altered yielding: β-turns, 3%; β-turns/loops, 8%; random coil, 34%; α-helix, 42%; and parallel β-sheet, 13%.

The concurrence between CD and FTIR results pinpoints the robustness of both deconvolution approaches, which can be affected, in the case of FTIR, by the iterative procedure carried out by the researcher (see Materials and Methods section). We could not use FTIR in the presence of the cation, since the addition of the ion caused protein precipitation, probably because of formation of several hydroxides with the Co^{2+}.[33]

To sum up, all the spectroscopic results indicate that GkNSAAR is mainly formed by α-helical structure and that the presence of the ion does not alter either its tertiary structure.

Stability of GkNSAAR Either in the Absence or in the Presence of Co^{2+}

On the basis of the spectroscopic results described, several questions can be raised: how stable is the native structure acquired above pH 6.0?; and although GkNSAAR does not acquire a native structure up to pH 6.0, have the species at low pH a well-folded conformation?, if so, how is their stability? Furthermore, do the changes observed upon ion addition result in stability variations? To address those questions, we carried out thermal and chemical denaturations in the presence and in the absence of the ion.

Thermal Denaturations. Thermal denaturations were followed by CD, FTIR, and fluorescence at several pH. They were not protein concentration-dependent, and they were irreversible at all pH, whether or not the ion was present. Then, we did not estimate the thermodynamic parameters governing the unfolding process.

The CD and fluorescence thermal scans at pH < 5.0, whether or not the ion was present, did not show a sigmoidal behavior (see Figure 4), suggesting that the species populated at those pH did not have a well-folded conformation. Above pH 5.0, an irreversible transition was observed by both techniques, with an apparent T_m close to 354 K; in the pH interval from 6.0 to 9.0, irreversible transitions with the same apparent thermal midpoint were observed. At pH > 10.0 no sigmoidal transition was observed (see Figure 4). The FTIR thermal denaturations were only carried out at pH 8.0, yielding a $T_m = 355.7 \pm 0.9$ K (data not shown), close to those obtained by CD and fluorescence.

Chemical Denaturations. Since the thermal denaturations were irreversible, thus precluding any reliable conclusions, we carried out chemical denaturations at pH 8.0. Upon addition of GdmCl to GkNSAAR, in the absence of the ion, we observed a shift in the emission maximum from 340 to 350 nm. The intensity at 340 nm decreased monotonically up to 2*M* GdmCl, where it reached a plateau to further

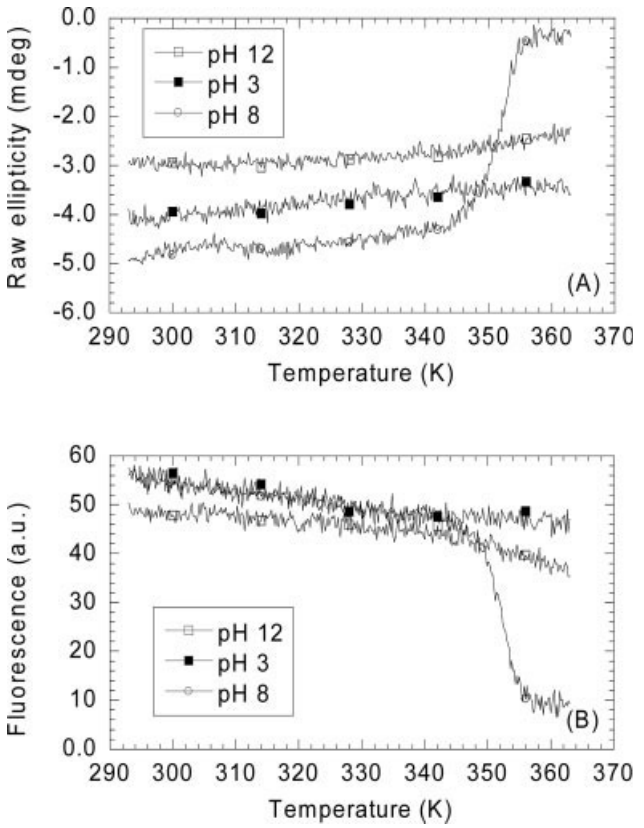

FIGURE 4 Thermal denaturations of GkNSAAR at several pH as determined by CD and fluorescence. A: Thermal denaturations followed by the changes in raw ellipticity at 222 nm at the selected pH. B: Thermal denaturations followed by the intrinsic emission fluorescence at 340 nm after excitation at 280 nm at the indicated pH. To allow for comparison among the three different pH in both techniques, the y-units in both panels are arbitrary.

decrease following a sigmoidal behavior (Figure 5A). The first monotonic transition was not observed by following the changes in the ellipticity at 222 nm (Figure 5B, filled squares). The first transition was concentration-dependent, indicating that it involves oligomer dissociation (Supporting Information Figure 2), but it was very flat to allow a good estimation of any chemical denaturation midpoint; conversely, the second one did not show any concentration-dependence, and it must involve unfolding of monomeric species. The first transition was not reversible, but the second one was reversible, and then, its *m*-values and chemical-denaturation midpoints (Table II) were determined.

We also followed the chemical-denaturations by monitoring: (i) the ANS fluorescence intensity; and (ii) the V_e in gel filtration experiments. In the ANS experiments, a large increase in the fluorescence intensity at 480 nm was observed (Figure 5C) at low GdmCl concentrations, to further decrease at higher denaturant concentrations. The gel filtration data indicate that between 0 and 2*M* of GdmCl (that is, where the first concentration-dependent transition is observed, Figure 5A), the V_e goes from 10.94 ml (at 0*M* GdmCl) to a broad peak centered at 10.0 ml (at 1.5*M* GdmCl) at 4 μM of protein concentration (data not shown). Taken together, these experimental results suggest that at such low [GdmCl]s, there are species with solvent-exposed hydrophobic patches (ANS), which could interact with the column (gel filtration).

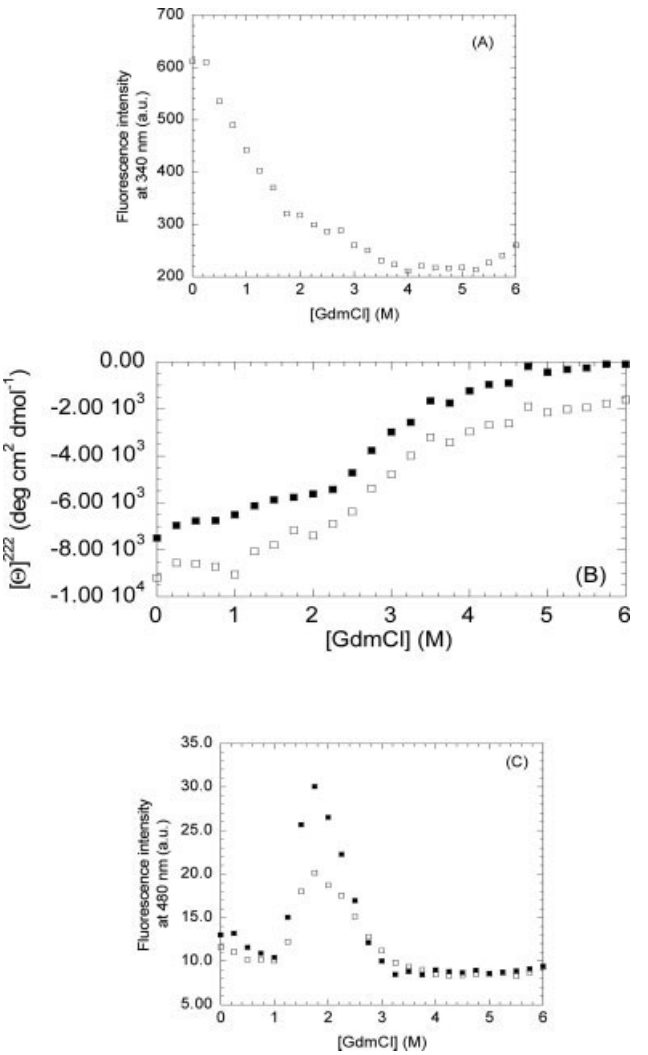

FIGURE 5 Stability of GkNSAAR determined by GdmCl-denaturations. A: The fluorescence intensity at 340 nm versus the [GdmCl] at pH 8.0 in the absence of Co^{2+}. Data were acquired at 4 μM of protein concentration at 298 K. B: The [Θ] at 222 nm at pH 8.0 in the absence (blank squares) and in the presence (filled squares) of the ion. The units on the *y*-axis are arbitrary. C: The fluorescence intensity at 480 nm in ANS fluorescence experiments versus the [GdmCl] at pH 8.0 in the absence (blank squares) and in the presence of Co^{2+} (filled squares). Data were acquired at 4 μM of protein concentration at 298 K.

Table II Thermodynamic Parameters of the Chemical Denaturation of GkNSAAR at pH 8.0 in the Absence and in the Presence of Co^{2+}[a]

	1 Day			10 Days		
	First Transition	Second Transition		First Transition	Second Transition	
Protein Concentration (μM)	$[GdmCl]_{1/2}$ (M)	m (kcal mol^{-1} M^{-1})	$[GdmCl]_{1/2}$ (M)	$[GdmCl]_{1/2}$ (M)	m (kcal mol^{-1} M^{-1})	$[GdmCl]_{1/2}$ (M)
1.0	Broad	2.2 ± 0.2 (2.0 ± 0.2)[b]	2.86 ± 0.04 (2.88 ± 0.06)[b]	Broad	2.5 ± 0.2	2.96 ± 0.04
4.0	Broad	2.1 ± 0.3 (1.7 ± 0.2)[b]	2.95 ± 0.03 (2.90 ± 0.08)[b]	Broad	2.3 ± 0.3	2.85 ± 0.08
10.0	Broad	3.0 ± 0.6	3.00 ± 0.08			
1.0[c]				Broad	2.1 ± 0.4	2.8 ± 0.1

[a] All experiments were carried out at 298 K. The values shown were obtained by following the changes in fluorescence intensity at 340 nm after excitation at 280 nm (similar results were obtained by excitation at 295 nm). Thermodynamic parameters were obtained by using a three-state equation in oligomeric proteins.[34] Errors are fitting errors to the three-state equation. The first transition was in all cases too broad to yield proper thermodynamic parameters (see Supporting Information Fig. 2 and Fig. 5).

[b] The value obtained in the presence of 0.5 mM of Co^{2+} is shown within parenthesis.

[c] Renaturation experiments were acquired after a 10-day incubation period at 278 K.

Chemical denaturations of GkNSAAR in the presence of the ion monitored by the fluorescence intensity show two transitions, identical to those observed in the absence of the ion. The first monotonic transition was concentration-dependent, but it was not reversible (data not shown), precluding any thermodynamic study. On the other hand, the second transition was reversible, but concentration-independent, yielding the same thermodynamic parameters as in the absence of the ion (Table II). Finally, the [Θ] at 222 nm showed, as in the absence of the ion, a single broad transition (Figure 5B, filled squares). Chemical denaturations followed by ANS fluorescence (Figure 5C, filled squares) showed the same tendency as in the absence of the ion. Either in the presence or in the absence of the ion, tetramer dissociation showed a hysteresis behavior (that is, the refolding equilibrium curve did not superimpose with the unfolding equilibrium one) precluding any thermodynamic study.

DISCUSSION

GkNSAAR is a Tetramer

The majority of the *N*-succinylamino acid racemases described to date are homooctamers or homohexamers, and then, GkNSAAR is one of the few racemases which shows a tetrameric structure.[8–14] The structures of the enolases reported so far from eukaryotic sources are usually dimeric, whereas the crystal structures of the bacterial enolases from *S. pneumoniae* and *En. hirae* show a tetrameric fold or a similar octameric association comprising a tetramer of dimers.[35,36] It has been suggested that changes in protein quaternary structure within the same family are associated to the evolution of new functions and regulation.[37]

In the following, we will try to explain the tetrameric quaternary structure of GkNSAAR based on: (i) the protein sequence; and (ii) the monomeric tertiary structure. First, we used the sequence of DrNSAAR, whose three-dimensional structure is known[14]; the sequence identity between both proteins is 45% (a similar percentage has also been observed with other NSAARs[18]) (Figure 6C). Recently, it has been shown that with sequence identities in the range of 30–40%, the conservation of the quaternary structure is ~70%.[37] The corresponding percentages for the twenty amino acids are similar for GkNSAAR and DrNSAAR, except for: (i) Ala and Gly, which are a 2% lower in GkNSAAR than in DrNSAAR; and (ii) Ile and Lys, which are a 2% higher in GkNSAAR than in DrNSAAR. Then, the *per* residue differences between both proteins are restricted to hydrophobic and charged residues; since the three-dimensional structure of DrNSAAR has revealed that the oligomeric interfaces are comprised of an extensive network of hydrophobic contacts,[14] these differences in a particular type of residue might hamper octameric formation.

And second, a structural model of GkNSAAR was generated using the 2.3 Å-resolution structure of DrNSAAR (PDB number: 1XPY).[14] DrNSAAR octameric oligomerization occurs mainly via three types of interactions. In the first one, each monomer packs tightly to form a dimer using an interface, which is highly conserved in GkNSAAR; this region is called the A1-C1 interface, following original nomenclature by Hsu and coworkers (Figures 6A and 6C, indicated by asterisks in the latter). This interface is comprised by α-heli-

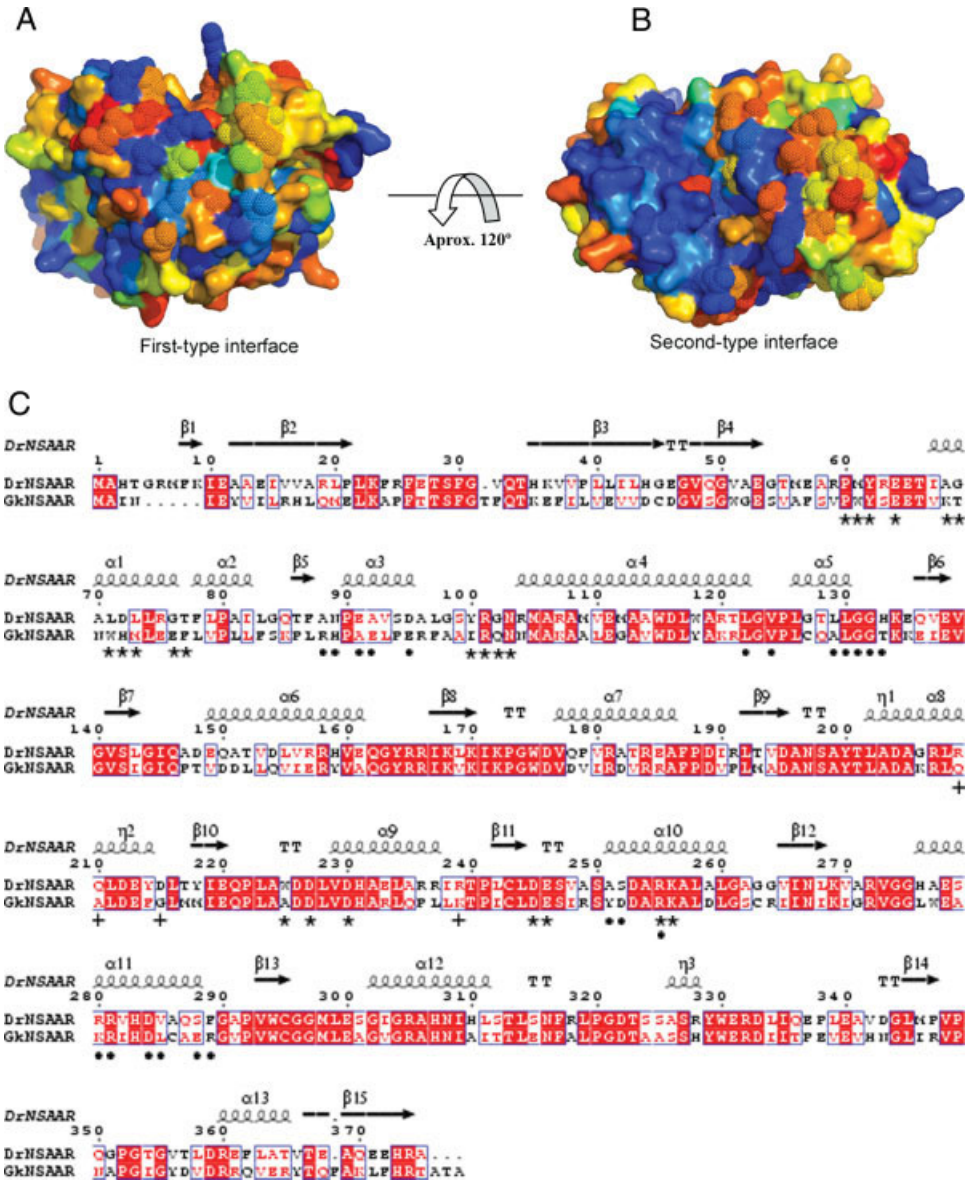

FIGURE 6 Molecular modeling of GkNSAAR. Molecular surface of the modeled GkNSAAR showing residue conservation of first (A) and second (B) type of interfaces from DrNSAAR.[14] The conservation score is color coded, going from dark blue (fully conserved) over light blue, green, yellow, and orange toward red (most variable). Counterpart residues for GkNSAAR interfaces are represented as dots. Sequence alignment was carried out with ClustalW,[38] which was the input to calculate conservation scores at each amino acid position in ConSurf.[39] For visualization, the conservation scores were written into the B-factor field of the GkNSAAR model coordinate file. (C) Sequence alignment generated with the Espript software[40] using the CLUSTALW alignment as input, together with PDB 1XPY. DrNSAAR residues involved in the different interfaces are represented as follows: A1-C1 (*), A2-C2 (•), and A1-A2-A4 (+).

ces, and the corresponding GkNSAAR residues involved are: Pro56, Tyr58, Arg97, Asp223, Asp227, Glu242, Arg251, and Lys252. The second type of interface (the so-called A1-C2 interface) allows tetramer formation in DrNSAAR, because of dimer association, and involves mainly α-helices. The conservation score for this interface in GkNSAAR is lower than for the first one, with the following residues involved in the main interactions: Arg251, Glu284 (Ser288 in DrNSAAR), Asp280, Arg277, and Lys276 (Arg280 in DrNSAAR) (Figures 6B and 6C, indicated by black dots in the latter). In DrNSAAR, the third type of interactions (A1-A2-A4) make the two tetramers (which are, in turn, composed by a four-

fold axis-related monomers) to be packed by residues Arg209, Gln210, Asp215, and Arg239. However, these residues do not have the corresponding counterpart in GkNSAAR (Figure 6C, indicated by crosses) and then, it would explain why the tetramer does not further oligomerize. Thus, the modeled structure suggests that: (i) hypervariability among helices, which otherwise do not seem to alter the structure of the isolated monomer (as shown by CD and FTIR); and (ii) the absence of the third octameric-stabilizing interface, are together responsible for the absence of the homooctamers in GkNSAAR. At this stage, it is important to pinpoint that even though there is a change in the quaternary structure, the largest oligomerization interfaces (the first two ones) are conserved. Finally, it is interesting to indicate that in additional sedimentation velocity experiments at pH 5.3 and 9.0, small populations of highly elongated homooctameric molecules were detected (data not shown). Although we have discussed above that homooctamer formation is not favored, it could be that at extreme pH, some groups titrate and/or some conformational changes occur (Figures 2A and 3B) allowing packing of a small population of the pre-existing tetramers in higher-order complexes.

Finally, it could be thought that the calculation of the corresponding Stokes radius of the tetrameric modeled structure by using HYDRPRO[41] and its comparison to that from a putative trimeric structure could further support the presence of tetrameric species in GkNSAAR. Trimeric and tetrameric models were manually built by superimposition with the 1XPY structure. The theoretical Stokes radii for the trimeric and tetrameric states calculated by using HYDROPRO[41] were 41.7 and 46.4 Å, respectively. The similarity between the value for that of the tetrameric species and that from gel filtration measurements (46.7 Å, see in Results section) further supports that the dominant species in solution is a tetramer.

Since the protein is a tetramer, is the structure of one of the protomers (from here, we will understand protomers as a monomer unit) similar to one of the protomers belonging to the homooctameric species observed in other family members? We have not been able to find good diffracting crystals for GkNSAAR so far, but the low resolution techniques used in this work, CD and FTIR, allow us to estimate the percentage of secondary structure of each monomer (Table I). The percentages of secondary structure in DrNSAAR are 32% for α-helix and 17% for β-sheet (either parallel or antiparallel), which are similar to those obtained experimentally by deconvoluting the CD spectra in GkNSAAR (Table I): 35 and 14% (the sum of 9 and 5 in such Table, the two types of β-sheet), respectively. Further similarities are found when the metal binding pocket is compared: the binding pocket of Mg^{2+} in DrNSAAR is relatively close to several Phe and Tyr amino acids,[14] which also seems to occur in the binding site of Co^{2+} in GkNSAAR. Then, we suggest that although the quaternary structure is not conserved among the NSAARs, the tertiary and secondary structures, and the surroundings of the metal binding site are preserved.

Cobalt Ions Only Alter Slightly the Secondary Structure of GkNSAAR

Metals perform a variety of tasks in cells from structural stabilization to enzyme catalysis, activating key life processes such as respiration and photosynthesis.[42] The Na, K, Mg, Ca, Zn, Cu, Fe, Co, and Mn ions are the most frequently found in proteins under physiological conditions. Since the first NSAAR was discovered in *Actinomycetes* strains,[9] it has been known that NSAARs are metalloenzymes. We have shown that GkNSAAR has the highest percentage of enzymatic activity in the presence of Co^{2+} [18] (which is the desired condition from a strict industrial point of view), and then, the studies of the conformational changes have been also carried out in the presence of that cofactor (for instance, in the presence of Mg^{2+} the activity was a 10% of that observed with Co^{2+}). These studies will allow us to evaluate the conditions under which GkNSAAR could be used in the synthesis of optically pure amino acids, together with a stereospecific L-acylase. In this work, we observed that the presence of the ion: (i) decreased the ellipticity in the far-UV CD spectrum (Figure 3A), and the percentage of helical structure as shown in Table I, but not the quaternary one (Figure 1A); (ii) did modify the asymmetric environment of the aromatic residues (Figure 3C); and (iii) did not alter substantially the chemical stability of the isolated monomeric forms (Table II). Thus, in contrast to other ions, such as Zn^{2+}, which can have dramatic effects in the structure of the proteins,[43,44] the cobalt ion does not alter significantly the structure of the GkNSAAR, nor does the solvent-exposure of hydrophobic polypeptide patches[45]; that is, Co^{2+} is necessary for the highest enzyme activity, but not for attaining the native-like protein scaffold nor its stability.

The pH-Denaturation of GkNSAAR Involves a Molten-Globule-Like Species at Low pH

The GkNSAAR shows a tetrameric structure (but not necessarily a native-like one) at least from pH 5.3 to 9.0 as shown by AU. At the acidic pH, gel filtration results suggest that the protein interacts with the column, because of the long elution volume. Taken together both results suggest that the quaternary fold acquired by the protein at pH 5.3 has some solvent-exposed regions, as it is also supported by ANS bind-

ing experiments (Figure 2B). It is interesting to note that at pH 5.5, the enzyme shows a 3% activity (when compared with pH 8.0) (Supporting Information Figure 3), thus supporting that the structure at that pH is not completely native-like (data not shown). We can describe how the functional structure is attained, based on the different spectroscopic techniques.

The acquisition of tertiary native-like structure (either in the presence or in the absence of the ion), from the acidic regions occurs at a pK_a of ~4.8 (Figure 2A) which is similar to that observed in an aspartic and/or glutamic residue[24]; interestingly enough, in the modeled structure the oligomerization interfaces are mainly formed by glutamic and aspartic residues, suggesting that the acquisition of quaternary and tertiary structure occurs concomitantly. A similar value was obtained by monitoring the ANS fluorescence.

The secondary structure (as monitored by far-UV CD) was not acquired until pH 7.0 (Figure 3B, filled squares). In the presence of the ion, the same tendencies are observed, except for the changes in far-UV (Figure 3B, blank squares), where no transition was observed. Since the pK_a of the transition in the absence of the ion, was close to that of a histidine residue (6.7 ± 0.1)[24] (Figure 3B, filled squares), we suggest that the conformational changes monitored by CD are related to the presence of a chelating histidine. Interestingly enough, histidine has been suggested to be involved in the enzymatic reaction of the enolase family.[14]

One question, however, must be answered: which is the conformational state populated at very low pH? Since the different protein species bound ANS (Figure 2B), and they did not show a sigmoidal thermal denaturation (see Figure 4), we suggest that the low-pH species is a molten-globule.[46] This species has at least some of the tryptophans still buried (as concluded from the blue-shifted fluorescence maxima at low pH, data not shown), but with a nonasymmetric environment for the majority of the aromatic residues (Figure 3D).

Equilibrium Unfolding of GkNSAAR Involves a Non-Native Monomeric Intermediate Whether or Not Cobalt Ions are Present

Most of the previous work on protein folding has focused on small single-domain proteins that fold rapidly and avoid aggregation.[47] However, there are many proteins in the cell which are large, with multiple folding domains and/or subunits, and which probably do not follow the simple folding principles established on results from small proteins. Further complications arise in multimeric proteins, where their folding reactions involve not only intramolecular interactions, but also intermolecular ones. How the amino acid sequence controls subunit–subunit interactions, and which additional stability is conferred by such contacts can be only addressed by characterizing the stability and conformational properties of multimeric proteins.[48] Moreover, the stability and folding mechanism of a protein can be altered by the presence of cofactors: it is estimated than more than 20% of all proteins in the cell coordinate cofactors in their native states to attain specific functions. The cofactor protein stabilization depends on the particular polypeptide chain; for instance, the cytochrome b562 of *Escherichia coli* is stabilized by 14 kJ mol^{-1} when the heme cofactor is present,[49] but the stability of the flavodoxin of *Desulfovibrio desulfuricans* is not affected by the presence of flavin.[50]

The chemical denaturation data (Supporting Information Figure 2) suggest that the first transition involves tetramer dissociation, M_4, toward a monomeric species, M: $M_4 \rightleftarrows 4M$, and the second one involves monomer unfolding (since, it is not concentration-dependent, Table II). The structure of the monomeric intermediate is non-native, because the CD signal changed concomitantly to the fluorescence spectra, either in the absence or in the presence of the ion (Figure 5B). Moreover, when GdmCl denaturation was followed by ANS fluorescence, a complete decrease in the intensity at 480 nm only occurred when the second transition had completely finished (i.e., at [GdmCl] $> 3M$) (Figure 5C), suggesting that the monomeric intermediate species have a large amount of solvent-exposed hydrophobic surface. Then, since this intermediate species is able to bind ANS and is monomeric, we hypothesize that its structure is similar to that of the molten-globule observed at low pH (see earlier).

Tetramer dissociation showed a hysteresis behavior, whether or not the ion was present, precluding any thermodynamic study. Hysteresis is due to the nonequivalence of the unfolding and refolding reactions. Then, the presence of the Co^{2+} in the refolding buffer is not enough to accomplish monomer assembly, even after long incubation times, probably due to the fact that Co^{2+} is not covalently bound to the protein. The absence of tight bonds would also explain why the chemical stability of the protein was not affected by the presence of the ion (see Figure 5). We do not know the exact reasons behind the hysteresis behavior of the dissociation step, but we speculate that since the monomer have two different interacting surfaces (see the Discussion of the modeled structure), docking of the two preformed monomers by the proper use of the correct surface might be highly hampered.

Energetics of the Chemical- and Thermal-Unfolding Reaction Compared with Other Proteins

Since the dissociation reaction was not reversible (and we have not been able to determine the dissociation constant of

the tetramer by AU), we could not estimate the oligomeric stability of GkNSAAR. The dissociation free energies of other oligomeric proteins are in the range of 37–250 kJ mol^{-1} of oligomer.[51,52] The free energy of unfolding of the monomeric GkNSAAR can be estimated to be 106 kJ mol^{-1} from the fitting of the first broad transition. This is just in the middle of the range observed for the free energy of dissociation of other proteins, which means that most of the global unfolding free energy of GkNSAAR originates within each monomer, and then, the interactions establishing the tetrameric scaffold, although they could be numerous, are relatively weak. This result also indicates that monomers are stable enough to exist isolated in solution under determined solvent conditions.

Although chemical denaturations had two transitions, thermal denaturations at any pH showed a single irreversible one, with a high apparent thermal midpoint (~354 K). The protein has a maximum enzymatic activity at 328 K, and the complete lost of enzymatic activity occurred over 353 K (data not shown); then, thermal enzymatic inactivation occurred because of thermal unfolding. However, why is GkNSAAR so thermostable? It has been suggested that the high-level of quaternary structure (the octameric species) is responsible for the extreme thermal stabilization of NSAARs[14] or other members of the enolase superfamily.[35] The quaternary structure of GkNSAAR and its high stability (354 K), the latter larger than that reported for DrNSAAR (343 K),[14] do not support that suggestion. On the other hand, a comparison among the sequences of proteins from thermophiles and mesophiles can shed some light on the origin of the thermostability of GkNSAAR.[53] Protein sequences from thermophiles show a large proportion of charged (Arg, Asp, Glu, and Lys) and hydrophobic (Gly, Ile, Pro, and Val) residues, and concomitantly, a low percentage of uncharged polar amino acids (Asn, Gln, and Thr). In GkNSAAR, the percentage of charged and hydrophobic residues accounts for a 50% of the total number of residues, and then, it is larger than that of uncharged ones (10%), suggesting that its sequence determines its thermostability, and also, as it has been previously discussed, its oligomerization state (see earlier). More detailed molecular interpretations on the stability of oligomeric proteins are difficult. Although there is a great deal of research these days into prediction of subunit affinities (as shown by the CAPRI results), accurate predictions remain elusive.[54] We can only hypothesize that the high stability of the GkNSAAR is important for its function, as it has been described recently in other high-order oligomeric proteins.[55]

CONCLUSIONS

The results in this work indicate that the native secondary structure of GkNSAAR at pH 8.0, the pH of maximal activity, is mainly formed by α-helix. The protein is a tetramer at pH 8.0; this functional structure is only stable within a very narrow pH range (from pH 7.0 to 9.0). Then, the possible industrial applications of GkNSAAR must keep in mind that slight changes in the acidic solution conditions result in conformational changes which reduce its activity. In GdmCl denaturation experiments, the folding reaction proceeds *via* a monomeric intermediate with non-native structure. Upon addition of 0.5 m*M* of Co^{2+}, the secondary structure of the protein changed slightly, as shown by CD and FTIR deconvoluted data, but the tertiary structure was not altered. Further, neither were the quaternary structure or the chemical stability modified by the presence of the metal. Then, although the largest enzyme activity is linked to the presence of the Co^{2+}, the ion seems to alter slightly the content of secondary structure.

MATERIALS AND METHODS

Materials

All the reagents and chemicals were from Sigma (USA) and of the highest purity available. The molecular mass marker was from GE Healthcare (USA). Ultra-pure urea and GdmCl were from ICN Biochemicals (USA). Exact concentrations of GdmCl were calculated from the refractive index of the solutions.[56] Dialysis tubing with a molecular weight cut-off of 3500 Da was from Spectrapore (UK). Water was deionized and purified on a Millipore system. Experiments in the presence of 0.5 m*M* of Co^{2+} were acquired by dissolving the proper amount of a 1*M* stock solution of $CoCl_2 \times 5H_2O$.

Protein Expression and Purification

GkNSAAR was expressed and purified as described.[18] The protein used in this work was not histidine-tagged; the tag was removed by thrombin cleavage following manufacturer instructions (GE Healthcare) to avoid possible interference during the stability studies in the presence of the ion. The protein is 379-residues long, and it contains 10 tyrosines and eight tryptophans. Protein purity was checked by SDS gel and mass spectrometry and in all preparations was larger than 95%. Activity of the protein used in the biophysical studies was tested as described elsewhere[18] (Supporting Information Figure 3). Although when the activity is substantially reduced, there is still a substantial amount of fluorescence (see for instance, at pH 10.5), and thus, a qualitative agreement exists between the bell-shaped curves of fluorescence intensity and pH-activity profile. Protein concentration was calculated based on the extinction coefficients of amino acids.[57]

Gel Filtration Chromatography

The standards used in column calibration, and their corresponding Stokes radii were: ovoalbumin (30.5 Å); bovine serum albumin (35.5 Å); aldolase (48.1 Å); ferritin (61 Å), and thyroglobulin (85 Å).[58,59] The bed and the void volumes were determined by using

riboflavin and blue-dextran, yielding 23.6 and 7.0 ml, respectively. Samples were loaded at 25 m*M* Tris (pH 7.3) with 150 m*M* NaCl at 1 ml min^{-1} in an analytical calibrated Superdex G200 HR 16/60 (GE Healthcare) column, running on an AKTA-FPLC system (GE Healthcare) at 298 K, and monitored with an on-line detector at 280 nm. Gel filtration chromatography was used to determine the hydrodynamic radius, R_s, of the protein, as it has been previously described.[60,61] Briefly, such approach uses the weight average partition coefficient (σ) of a protein and takes the error function complement of σ, ($\mathrm{erfc}^{-1}(\sigma)$]) which has a linear relationship with the molecular Stokes radius, R_s[60]:

$$R_s = a + b\left(\mathrm{erfc}^{-1}(\sigma)\right).$$

where a and b are the particular calibration constants for the column.

The buffers at the different pH (see latter) were used at a final concentration of 50 m*M*, with 150 m*M* of NaCl to avoid column interactions. Each measurement was repeated three times using a 2.75 μM protein concentration. Protein concentration ranged from 1 to 76.45 μM in experiments aimed to determine the association constant.

Analytical Utracentrifugation

Sedimentation equilibrium experiments were performed at 298 K in an Optima XL-A (Beckman-Coulter Inc.) analytical ultracentrifuge equipped with UV-visible optics, using an An50Ti rotor, with a 3 mm double-sector charcoal-filled Epon centerpiece. Samples of freshly dialyzed protein at 15 μM in 20 m*M* Tris-HCl (pH 8.0) were loaded into the cell, and the dialysate was transferred to the reference sector. The velocities used were 3000 (10,920 g), 6000 (21,840 g), 8000 (29,120 g), 10,000 (36,400 g), and 42,000 (152,880 g) rpm. Short column (23 μl) low speed sedimentation equilibrium was performed at 6000–8000 rpm, and the system was assumed to be at equilibrium when the successive scans overlaid. The equilibrium scans were obtained at 280 nm. The baseline signal was measured after high speed centrifugation (5 h at 42,000 rpm). The whole-cell apparent molecular weight of the protein was obtained with the program EQASSOC,[19] and the goodness of the fitting was judged by the values of residuals (in all cases within less than ± 0.02) (Figure 1B). Experiments were also acquired at pH 5.3 (50 m*M*, acetic acid) and pH 9.0 (50 m*M*, Tris).

Fluorescence Measurements

Fluorescence spectra were collected on a Cary Varian spectrofluorimeter (Varian, USA), interfaced with a Peltier unit, at 298 K. The GkNSAAR concentration in the pH- or chemical-denaturation experiments was 1 μM, unless it is stated; the final concentrations of the buffers were, in all cases, 10 m*M*. A 1-cm-pathlength quartz cell (Hellma) was used.

Steady State Spectra. Protein samples were excited at 280 and 295 nm to characterize a different behavior of tryptophan and tyrosine residues. The slit widths were 5 nm for the excitation and emission lights. The fluorescence experiments were recorded between 300 and 400 nm. The signal was acquired for 1 s and the wavelength increment was set to 1 nm. Blank corrections were made in all spectra.

The sample pH were measured after completion of the experiments. The pH was measured with a thin Aldrich electrode in a Radiometer (Copenhagen) pH-meter. The salts and acids used were: pH 2.0–3.0, phosphoric acid; pH 3.0–4.0, formic acid; pH 4.0–5.5, acetic acid; pH 6.0–7.0, NaH_2PO_4; pH 7.5–9.0, Tris acid; pH 9.5–11.0, Na_2CO_3; pH 11.5–12.0, Na_3PO_4.

ANS-Binding. Excitation wavelength was 380 nm, and fluorescence emission was measured from 400 to 600 nm. Slit widths were 5 nm for excitation and emission light. Stock solutions of ANS (1 m*M*) were prepared in water and diluted to yield a final concentration of 100 μM. Blank solutions were subtracted from the corresponding spectra.

Thermal Denaturation Experiments. Excitation wavelength was either 280 or 295 nm, and fluorescence emission was collected at 340 nm. Slit widths were 5 nm for excitation and emission light. Thermal scans were acquired every 0.2 K and the heating rate was 60 K h^{-1}.

Circular Dichroism Measurements

Circular dichroism spectra were collected on a Jasco J810 spectropolarimeter (Japan) fitted with a thermostated cell holder and interfaced with a Peltier unit. The instrument was periodically calibrated with (+) 10-camphorsulphonic acid.

Steady-State Spectra. Isothermal wavelength spectra at different pH were acquired at a scan speed of 50 nm min^{-1} with a response time of 4 s and averaged over four scans, at 298 K. Far-UV measurements were carried out at 1 μM of protomer concentration, 10 m*M* of the corresponding buffer (see earlier), in a 0.1-cm-pathlength cell. Blank corrections, either in the presence or in the absence of the ion, were acquired in all experiments. Every pH-denaturation experiment was repeated three times with new samples. Near-UV measurements were carried out at a protein concentration of 15 μM, in a 0.5-cm-pathlength cell. Molar ellipticity, [Θ], was obtained from raw ellipticity data, Θ, as described.[61]

In the GdmCl denaturation experiments, far-UV CD spectra were acquired with a scan speed of 50 nm min^{-1}; four scans were recorded and averaged, with a response time of 4 s, at 298 K. The cell pathlength was 0.1 cm, with a protomer concentration of 1 μM, unless it is stated. Spectra were corrected by subtracting the proper baseline. Every chemical denaturation experiment was repeated three times with new samples.

Thermal Denaturation Experiments. Thermal denaturations at several pH were performed at heating rates of 60 K h^{-1}, and a response time of 8 s. Thermal scans were collected in the far-UV region at 222 nm in 0.1-cm-pathlength cells with a total protein concentration of 1 μM. The possibility of drifting of the spectropolarimeter was tested by running two samples containing buffer, before and after the thermal experiments. No difference was observed between the scans.

Fourier Transform Infrared Spectroscopy

The protein was lyophilized and dissolved in deuterated buffer at the desired pH in D_2O; no pH-corrections were done for the isotope effects. Samples of GkNSAAR, at a final concentration of 125 μM, were placed between a pair of CaF_2 windows separated by a 50-μm thick spacer, in a Harrick demountable cell. Spectra were acquired on a Bruker FTIR instrument equipped with a DTGS detector and thermostated with a Braun water bath at the desired temperature. The cell container was filled with dry air.

Steady-State Spectra. Five-hundred scans *per* sample were taken, averaged, apodized with a Happ-Genzel function, and Fourier transformed to give a final resolution of 2 cm^{-1}. The signal-to-noise ratio of the spectra was better than 10,000:1. Buffer contributions were subtracted, and the resulting spectra were used for analysis. To determine the amount of the secondary structure components, the Amide I′ band in D_2O was decomposed into its constituents by curve-fitting (with a combination of Gaussian and Lorentzian functions), by means of the number and position of bands obtained from the deconvolved (with a Lorentzian bandwidth of 18 cm^{-1} and a resolution enhancement factor of 2) and the Fourier derivative (using a power of 3 and a breakpoint of 0.3) spectra. Band decomposition of the original Amide I′ has been described previously.[62–64] Briefly, for each component of the band, four parameters are considered: band position, band height, bandwidth, and band shape. Thus, in a typical Amide I′ band decomposition with six or seven band components, the number of parameters to fit is 24–28. The number and position of component bands is obtained through deconvolution and derivation, initial heights are set to 90% of those in the original spectrum for the bands in the wings and for the most intense component; and to 70% of the original intensity for the other bands. Initial bandwidths are estimated from the Fourier derivative; the Lorentzian component of the bands is initially set at 10%. The baseline is removed prior to starting the fitting process. The iteration procedure is carried out in two steps as described.[64] The mathematical solution of the decomposition may not be unique, but if restrictions are imposed, such as: (a) the maintenance of the initial band positions in an interval of ± 2 cm^{-1}; (b) the preservation of the bandwidth within the expected limits; or (c) the agreement with theoretical boundaries or predictions, the result becomes, in practice, unique. The fitting result is then evaluated by: (a) overlapping of the reconstituted overall curve on the original spectrum; and (b) examining the residuals obtained by subtracting the fitting from the original curve. The methodology has also been tested with well-characterized globular proteins. Besides, in some proteins whose structure was resolved by X-ray diffraction after obtaining the secondary structure by FTIR, a good agreement between the results from both techniques was observed.[65,66] The Supporting Information Figure 4 shows a typical deconvoluted FTIR band for GkNSAAR, in the absence of the ion.

The error in estimation of the percentage of secondary structure depends on several factors, such as the noise,[67] the parameters used for the deconvolution, the least-square method of fitting (which depends to some extent of the input parameters), or even the fact that each frequency (peak) is assigned to a single element of secondary structure (see the work of Homblé and coworkers for a detailed discussion on the factors affecting the percentages of secondary structure obtained by FTIR[68]). These factors can explain the differences among the values obtained by CD and FTIR in GkNSAAR (Table I) (and even, the CD deconvolution procedure is affected by similar technical and methodological problems[30]).

We also tried to subtract the side chain contributions from the original spectra (Supporting Information Figure 4) by using the procedure developed by the groups of Ruysschaert and Gerwert,[69,70] but in our hands, such procedure introduced distortions in the base line of the spectra yielding poor fitting results (data not shown).

Thermal Denaturation Measurements. The samples were submitted to heating cycles at each temperature. The heating cycles include: (i) a step-like increase in temperature; (ii) a stabilization period of the sample (or plain buffer) in the cell at each temperature; and (iii) a period of spectral acquisition. The duration of a complete heating cycle was ~2.5 h, in which the temperature was increased by approximately 5 K steps every 13 min. Fifty scans *per* temperature were averaged.

Analysis of the pH-, Chemical- and Thermal Denaturation Curves, and Free Energy Determination

The pH-denaturation data were analyzed assuming that both species, protonated and deprotonated, contributed to the (either fluorescence or CD) spectra. The acid-base equilibrium equation was used in the fitting of pH-denaturation data[61]:

$$X = \frac{\left(X_a + X_b 10^{(\mathrm{pH}-\mathrm{p}K_a)}\right)}{\left(1 + 10^{(\mathrm{pH}-\mathrm{p}K_a)}\right)},$$

where X is the physical property measured (ellipticity or fluorescence intensity), X_a is the one at low pH (acid form), X_b is that at high pH (basic form), and pK_a is the apparent pK of the titrating group. The apparent pK_a reported was obtained from three different measurements, carried out with fresh new samples.

The GdmCl-denaturation curves were analyzed as described in other three-state oligomeric proteins.[34] Thermal denaturation data were analyzed using a concentration-dependent two-state unfolding mechanism to obtain the T_m, where it was possible[34]; this value was used only in a qualitative manner, and it does not imply that the rest of the thermodynamic parameters can be obtained, since denaturations were irreversible at all pH explored. Fitting was carried out by using Kaleidagraph (Abelbeck software) working on a PC computer. When it was necessary, global fitting of the curves obtained by different techniques was carried out with MATLAB.

Modeling and Sequence Analysis Studies

The GkNSAAR structural model was obtained with the Swiss-model server,[71,72] using the structure of DrNSAAR (PDB number: 1XPY) as template, which has been solved at 2.3 Å resolution.[14] The stereochemical geometry of the final model was validated by PROCHECK.[73] Manual model building of the structures was performed with Swiss PDB viewer[71] and PyMOL.[74] The conservation of each residue among GkNSAAR and DrNSAAR was carried out using as input the sequence alignment calculated with ClustalW,[38] and the model generated by the Swiss-model server into the ConSurf server.[39] For visualization, the conservation scores were written into

the B-factor field of the GkNSAAR model coordinate file. An overall average G factor of −0.2 was observed (G factor scores should be larger than −0.5). Ramachandran plot statistics showed that 98.7% of the main-chain dihedral angles are found in the most favorable regions (data not shown). To estimate the theoretical Stokes radii of a trimeric and tetrameric species, models were obtained manually with Swiss PDB viewer,[71] by using the fit command on the individual monomeric model of GkNSAAR over the real octameric structure of DrNSAAR. After energy minimization of the models with the same software, HYDROPRO[41] was used to calculate their R_S.

The authors thank the reviewers for helpful comments, calculations, insights, and suggestions. They thank Prof. Alfred Wittinghofer for editing the manuscript, and for his patience and help. They also thank Dr. Javier Gomez (IBMC-UMH) for helpful insights and discussion, Dr. José A. Encinar (IBMC-UMH) for his help with FTIR calculations, and Mr. Jörn Güldenhaupt (Bochum, Germany) for providing the FTIR spectra of side chains contribution. They extend their thanks to Pedro Madrid Romero, May García, María del Carmen Fuster, and Javier Casanova for excellent technical assistance.

REFERENCES

1. Bommarius, A. S.; Schwarm, M.; Drauz, K. J. Mol Catal B Enzym 1998, 5, 1–11.
2. Breuer, M.; Ditrich, K.; Habicher, T.; Hauer, B.; Keßeler, M.; Stürmer, R.; Zelinski, T. Angew Chem Int Ed 2004, 43, 788–824.
3. Clemente-Jiménez, J. M.; Martínez-Rodríguez, S.; Rodríguez-Vico, F.; Las Heras-Vázquez, F. J Recent Pat Biotechnol 2008, 2, 35–46.
4. Wolf, L. B.; Sonke, T.; Tjen, K. C. M. F.; Kaptein, B.; Broxterman, Q. B.; Schoemaker, H. E.; Rutjes, F. P. J. T. Adv Synth Catal 2001, 343, 662–667.
5. Asano, Y. In D-Amino Acids: A New Frontier in Amino Acid and Protein Research-Practical Methods and Protocols; Konno, R.; Brückner, H.; D'Aniello, A.; Fisher, G. H.; Fujii, N.; Homma, H., Eds.; Nova Biomedical Books: New York, 2007; pp 579–589.
6. May, O.; Verseck, S.; Bommarius, A.; Drauz, K. Org Process Res Dev 2002, 6, 452–457.
7. Sakai, A.; Xiang, D. F.; Xu, C.; Song, L.; Yew, W. S.; Raushel, F. M.; Gerlt, J. A. Biochemistry 2006, 45, 4455–4462.
8. Tokuyama, S.; Miya, H.; Hatano, K.; Takahashi T. Appl Microbiol Biotechnol 1994, 40, 835–840.
9. Tokuyama, S.; Hatano, K.; Takahashi, T. Biosci Biotech Biochem 1994, 58, 24–27.
10. Tokuyama, S.; Hatano K. Appl Microbiol Biotechnol 1995, 42, 853–859.
11. Tokuyama, S.; Hatano K. Appl Microbiol Biotechnol 1995, 42, 884–889.
12. Verseck, S.; Bommarius, A.; Kula, M.-R. Appl Microbiol Biotechnol 2001, 55, 354–361.
13. Su, S. C.; Lee, C. Y. Enzyme Microb Technol 2002, 30, 647–655.
14. Wang, W. C.; Chiu, W. C.; Hsu, S. K.; Wu, C. L.; Chen, C. Y.; Liu, J. S.; Hsu, W. H. J Mol Biol 2004, 342, 155–169.
15. Demirjian, D. C.; Moris-Varas, F.; Cassidy, C. S. Curr Opin Chem Biol 2001, 5, 144–151.
16. Becker, P.; Abu-Reesh, I.; Markossian, S.; Antranikian, G.; Märkl, H. Appl Microbiol Biotechnol 1997, 48, 184–190.
17. Takami, H.; Takaki, Y.; Chee, G.-J.; Nishi, S.; Shimamura, S.; Suzuki, H.; Matsui, S.; Uchiyama, I. Nucleic Acids Res 2004, 32, 6292–6303.
18. Pozo-Dengra, J.; Martínez-Gómez, A.; Martínez-Rodríguez, S.; Clemente-Jiménez, J. M.; Rodríguez-Vico, F.; Las Heras-Vázquez, F. J Process Biochem, in press.
19. Minton, A. P. In Modern Analytical Ultracentrifugation; Schuster, T. M.; Laue, T. M., Eds.; Birkhäuser: Boston, MA, 1994; pp 81–93.
20. Cantor, C. R.; Schimmel, P. R. Biophysical Chemistry. W. H. Freeman: New York, 1980; Vol. 3.
21. Schuck, P. In Analytical Ultracentrifugation (Techniques and Methods); Scott, D. J., Harding, S. E.; Rowe, A. J., Eds.; RSC: Cambridge, UK, 2006; pp 15–140.
22. Lebowitz, J.; Lewis, M. S.; Schuck, P. Protein Sci 2002, 11, 2067–2079.
23. Burstein, E. A.; Vedenkina, N. S.; Ivkova, M. N. Photochem Photobiol 1973, 18, 263–279.
24. Thurlkill, R. L.; Grimsley, G. R.; Scholtz, J. M.; Pace, C. N. Protein Sci 2006, 15, 1214–1218.
25. Semisotnov, G. V.; Rodionova, N. A.; Razgulyaev, O. I.; Uversky, V. N.; Gripas, A. F.; Gilmanshin, R. I. Biopolymers 1991, 31, 119–128.
26. Woody, R. W. Methods Enzymol 1995, 246, 34–71.
27. Kelly, S. M.; Price, N. C. Curr Prot Pept Sci 2000, 1, 349–384.
28. Freskgård, P.-O.; Mårtensson, L.-G.; Jonasson, P.; Jonsson, B.-H.; Carlsson, U. Biochemistry 1994, 33, 14281–14288.
29. Vuilleumier, S.; Sancho, J.; Loewenthal, R.; Fersht, A. R. Biochemistry 1993, 32, 10303–10313.
30. Bohm, G.; Muhr, R.; Jaenicke, R. Protein Eng 1992, 5, 191–195.
31. Barth, A.; Martin, S. R.; Bayley, P. M. Biopolymers 1998, 45, 493–501.
32. Elfrink, K; Ollesch, J.; Stöhr, J.; Willbold, D.; Riesner, D.; Gerwert, K. Proc Natl Acad Sci USA 2008, 105, 10815–10819.
33. Rubinson, J. F.; Rubinson, K. A. Contemporary Chemical Analysis, 5th ed.; Prentince Hall: New Jersey, 2000.
34. Backmann, J.; Schäfer, G.; Wyns, L.; Bönisch, H. J Mol Biol 1998, 284, 817–833.
35. Yamamoto, H.; Kunishima, N. Act Crystallogr Section F 2008, F64, 1087–1090.
36. Gulick, A. M.; Palmer, D. R. J.; Babbitt, P. C.; Gerlt, J. A.; Ryament, I. Biochemistry 1998, 37, 14358–14368.
37. Levy, E. D.; Erba, E. B.; Robinson, C. V.; Teichmann, S. A. Nature 2008, 453, 1262–1265.
38. Thompson, J. D.; Higgins, D. G.; Gibson, T. J. Nucleic Acids Res 1994, 22, 4673–4680.
39. Armon, A.; Graur, D.; Ben-Tal, N. J Mol Biol 2001, 307, 447–463.
40. Gouet, P.; Courcelle, E.; Stuart, D. I.; Metoz, F. Bioinformatics 1999, 15, 305–308.
41. García de la Torre, J.; Huertas, M. L.; Carrasco, B. Biophys J 2000, 78, 719–730.
42. Thomson, A. J.; Gray, H. B. Curr Opin Chem Biol 1998, 2, 155–158.
43. Yi, S.; Boys, B. L.; Brickenden, A.; Konermann, L.; Choy, W. Y. Biochemistry 2007, 46, 13120–13130.
44. Park, P. S.-H.; Sapra, K. T.; Kolinski, M.; Filipek, S.; Palczewski, K.; Muller, D. J. J Biol Chem 2007, 282, 11377–11385.

45. Babor, M.; Greenblatt, H. M.; Edelman, M.; Sobolev, V. Proteins 2005, 59, 221–230.
46. Ptitsyn, O. B. Adv Protein Chem 1995, 47, 83–229.
47. Jackson, S. E. Fold Des 1998, 3, R81–R91.
48. Rumfeldt, J. A. O.; Stathopulos, P. B.; Chakaravarty, A.; Lepock, J. R.; Meiering, E. M. J Mol Biol 2006, 355, 106–123.
49. Robinson, C. R.; Liu, Y.; Thomson, J. A.; Sturtevant, J. M.; Sligar, S. G. Biochemistry 1997, 36, 16141–16146.
50. Apiyo, D.; Guidry, J.; Wittung-Stafshede, P. Biochim Biophys Acta 2000, 1479, 214–224.
51. Catanzano, F.; Graziano, G.; De Paola, B.; Barone, G.; D'Auria, S.; Rossi, M.; Nucci, R. Biochemistry 1998, 37, 14484–14490.
52. Sinha, S.; Mitra, N.; Kumar, G.; Bajaj, K.; Surolia, A. Biophys J 2005, 88, 1300–1310.
53. Chakravarty, S.; Varadarajan, R. FEBS Lett 2000, 470, 65–69.
54. Lensink, M. F.; Mendez, R.; Wodak, S. J. Proteins 2007, 69, 704–718.
55. Franco, J.; Bañuelos, S.; Falces, J.; Muga, A.; Urbaneja, M. A. Biochemistry 2008, 47, 7954–7962.
56. Pace, C. N. Methods Enzymol 1986, 131, 266–280.
57. Pace, C. N.; Scholtz, J. M. In Protein Structure, 2nd Ed.; Creighton, T. E., Ed.; Oxford University Press: Oxford, 1997; pp 253–259.
58. Hinkle, A.; Goranson, A.; Butters, C. A.; Tobacman, L. S. J Biol Chem 1999, 274, 7157–7164.
59. Carvalho, A. F.; Costa-Rodrigues, J.; Correia, I.; Costa-Pessoa, J. C.; Faria, T. Q.; Martins, C. L.; Fransen, M.; Sá-Miranda, C.; Azevedo, J. E. J Mol Biol 2006, 356, 864–875.
60. Darlin, P. J.; Holt, J. M.; Ackers, G. K. Biochemistry 2000, 39, 11500–11507.
61. Muro-Pastor, M. I.; Barrera, F. N.; Reyes, J. C.; Florencio, F. J.; Neira, J. L. Protein Sci 2003, 12, 1443–1454.
62. Arrondo, J. L. R.; Muga, A.; Castresana, J.; Goñi, F. M. Prog Biophys Mol Biol 1993, 59, 23–56.
63. Arrondo, J. L. R.; Castresana, J.; Valpuesta, J. M.; Goñi, F. M. Biochemistry 1994, 33, 11650–11655.
64. Bañuelos, F.; Arrondo, J. L. R.; Goñi, F. M.; Pifat, G. J Biol Chem 1995, 270, 9192–9196.
65. Echabe, I.; Haltia, T.; Freire, E.; Goñi, F. M.; Arrondo, J. L. R. Biochemistry 1995, 34, 13565–13569.
66. Encinar, J. A.; Molina, M. L.; Poveda, J. A.; Barrera, F. N.; Renart, M. L.; Fernández, A. M.; González-Ros, J. M. FEBS Lett 2005, 579, 5199–5204.
67. Echabe, I.; Encinar, J. A.; Arrondo, J. L. R. Biospectroscopy 1997, 3, 469–475.
68. Homblé, F.; Rausssens, V.; Ruysschaert, J. M.; Grouzis, J.-P.; Goormaghtigh, E. Biospectroscopy 1996, 2, 193–203.
69. Goormaghtigh, E.; Raussens, V.; Ruysschaert, J. M. Biochim Biophys Acta 1999, 1422, 105–185.
70. Güldenhaupt, J.; Adigüzel, Y.; Kuhlmann, J.; Waldmann, H.; Kötting, C.; Gerwert, K. FEBS J 2008, 275, 5910–5918.
71. Schwede, T.; Kopp, J.; Guex, N.; Peitsch, M. C. Nucleic Acids Res 2003, 31, 3381–3385.
72. Guex, N.; Peitsch, M. C. Electrophoresis 1997, 18, 2714–2723.
73. Laskowski, R. A.; MacArthur, M. W.; Moss, D. S.; Thornton, J. M. J Appl Crystallogr 1993, 26, 283–291.
74. DeLano, W. L. The PyMOL Molecular Graphics System on World Wide Web. Available at: http://www.pymol.org, assessed 2002.

Reviewing Editor: Alfred Wittinghofer